CHEMISTRY
A EUROPEAN JOURNAL

DOI: 10.1002/chem.201000489

# Mechanism of the Catalytic Deperoxidation of *tert*-Butylhydroperoxide with Cobalt(II) Acetylacetonate

**Natascia Turrà,[a] Ulrich Neuenschwander,[a] Alfons Baiker,[a] Jozef Peeters,[b] and Ive Hermans*[a]**

**Abstract:** The $Co^{II}/Co^{III}$-induced decomposition of hydroperoxides is an important reaction in many industrial processes and is referred to as deperoxidation. In the first step of the so-called Haber–Weiss cycle, alkoxyl radicals and $Co^{III}$–OH species are generated upon the reaction of the $Co^{II}$ ion with ROOH. The catalytic cycle is closed upon the regeneration of the $Co^{II}$ ion through the reaction of the $Co^{III}$–OH species with a second ROOH molecule, thus producing one equivalent of the peroxyl radicals. Herein, the deperoxidation of *tert*-butylhydroperoxide by dissolved cobalt(II) acetylacetonate is studied by using UV/Vis spectroscopy in situ with a noninteracting solvent, namely, cyclohexane. Kinetic information extracted from experiments, together with quantum-chemical calculations, led to new mechanistic hypotheses. Even under anaerobic conditions, the Haber–Weiss cycle initiates a radical-chain destruction of ROOH propagated by both alkoxyl and peroxyl radicals. This chain mechanism rationalizes the high deperoxidation rates, which are directly proportional to the cobalt concentration up to approximately 75 μM at 333 K. However, at higher cobalt concentrations, a remarkable decrease of the rate is observed. The hypothesis put forward herein is that this remarkable autoinhibition effect could be explained by the hitherto overlooked chain termination of two $Co^{III}$–OH species. The direct competition between the first-order Haber–Weiss initiation and the second-order termination can indeed explain this peculiar kinetic behavior of this homogeneous deperoxidation system.

**Keywords:** autoxidation · inhibitors · initiation · kinetics · peroxides

## Introduction

Alkylhydroperoxides (ROOH) are important intermediates and reactants (i.e., oxidants) in many oxidation processes.[1–4] For instance, in the industrial autoxidation of hydrocarbons, ROOH is formed in the reaction of peroxyl radicals (ROO•) with the substrate (RH) and can in turn be (partially) converted into an alcohol (ROH) and a ketone (Q=O) upon abstraction of its weakly bonded α-H atom by ROO•.[5–8] In many cases, the products of interest are the Q=O and ROH molecules (e.g., KA oil from the oxidation of cyclohexane; 6 Mt $a^{-1}$) rather than ROOH.[9,10] Industrial autoxidation processes are therefore often followed by subsequent deperoxidation in the absence of oxygen, thus converting the (remaining) ROOH intermediate into additional ROH and Q=O species. In other cases, such as the Amoco process in which *p*-xylene is oxidized to terephthalic acid (44 Mt $a^{-1}$), deperoxidation is carried out simultaneously with aerobic autoxidation. Cobalt complexes that are soluble in the reaction mixture are used for this purpose (i.e., homogeneous catalysis).[3] During this peroxide activation reaction, several reactive oxidizing species (i.e., oxygen-centered radicals) are generated, thus explaining why ROOH can also be used as an oxidant in metal-catalyzed (ep)oxidations.[11] The cobalt-induced cleavage of ROOH is also an important step in the (chemical) drying of alkyd paint.[12] Indeed, the spontaneous aerobic oxidation of binder molecules containing unsaturated C=C bonds (fatty acid chains) produces allylic hydroperoxides, the cobalt-induced decomposition and subsequent chemistry of which causes cross-linking between the binder molecules, thus shortening the drying time.

[a] N. Turrà, U. Neuenschwander, Prof. Dr. A. Baiker, Prof. Dr. I. Hermans
Department of Chemistry and Applied Biosciences
ETH Zürich, Wolfgang-Pauli-Strasse 10
8093 Zürich (Switzerland)
Fax: (+41) 44-633-1514
E-mail: hermans@chem.ethz.ch

[b] Prof. Dr. J. Peeters
Department of Chemistry
K.U.Leuven, Celestijnenlaan 200F
3001 Heverlee (Belgium)

Supporting information for this article is available on the WWW under http://dx.doi.org/10.1002/chem.201000489.

According to previous reports, cobalt ions react with ROOH in a so-called Haber–Weiss catalytic cycle [reactions (1) and (2)], thus resulting in an overall conversion of two ROOH molecules in alkoxyl ($RO^{\bullet}$) and peroxyl ($ROO^{\bullet}$) radicals [reaction (3)].[13,14]

$$Co^{II} + ROOH \rightarrow Co^{III}{-}OH + RO^{\bullet} \quad (1)$$

$$Co^{III}{-}OH + ROOH \rightarrow Co^{II} + H_2O + ROO^{\bullet} \quad (2)$$

$$2\,ROOH \rightarrow RO^{\bullet} + ROO^{\bullet} + H_2O \quad (3)$$

According to this two-step mechanism, the $Co^{II}$ ion is first oxidized by ROOH to a $Co^{III}$–OH intermediate, which can be regenerated back to the starting $Co^{II}$ ion upon reaction with a second ROOH molecule. At the moment, there is disagreement over which step [i.e., reaction (1) or (2)] is the rate-determining step, and hence which cobalt species (i.e., $Co^{II}$ or $Co^{III}$–OH) is the dominant in solution.[15,16] Little information is available on the precise rate or temperature dependence of the reactions. There is even controversy about the active species, that is, the monomeric or μ-oxo/μ-hydroxo-bridged species.[17] The mechanism has not been unambiguously clarified. A solid mechanistic understanding of the chemistry would be useful to guide process optimization and the development of more efficient (heterogeneous) catalytic systems.[18–20]

Herein, the deperoxidation of *tert*-butylhydroperoxide (denoted below as ROOH) by the homogeneous model catalyst cobalt(II) acetylacetonate ($[Co(acac)_2]$) is kinetically characterized in a noninteracting solvent, namely, cyclohexane. The main goal of this contribution is to quantify the kinetics and to gain insight into the fundamental chemistry of this reaction.

## Results and Discussion

**Introduction to the experiments**: *tert*-Butylhydroperoxide (5.5 M in decane, dried over molecular sieves (4 Å)) was used as a model hydroperoxide because of its lack of an α-H atom, the abstraction of which could significantly complicate the chemistry. Because hydroperoxides can form double H-bonded dimers,[21] the ROOH concentration was chosen to be low enough so that the population of the dimers can be neglected in the studied temperature range. Indeed, the dimers might have a different reactivity to the monomers. In the case of *tert*-butylhydroperoxide, the MPW1B95/6-31+G(d,p)[22] predicted zero-point-energy (ZPE)-corrected stability of the dimer at 0 K was 8 kcal $mol^{-1}$ with respect to the separated monomers. This finding implies that for the ROOH concentrations used in this study (i.e., below 10 mM), the dimer fraction can be neglected, even at a temperature as low as 323 K. For the same reason, ROOH was diluted in a noninteracting solvent (i.e., cyclohexane).

Although the precise deperoxidation rate was unknown at the start of this study, it can be anticipated that the reaction must be fast, even at room temperature (compare with the paint-drying process). Off-line analysis (e.g., by conventional gas chromatography) could therefore generate less-reliable kinetic data; therefore, the reaction should preferably be monitored in situ. Given the low catalyst and substrate concentrations, sensitive UV/Vis spectroscopy was selected to follow the reaction (see the Experimental Section).

**Spectral observations**: The UV/Vis spectrum of $[Co(acac)_2]$ in cyclohexane shows a broad absorption band between $\lambda =$ 250 and 320 nm and a weak feature at $\lambda = 225$ nm (Figure 1).

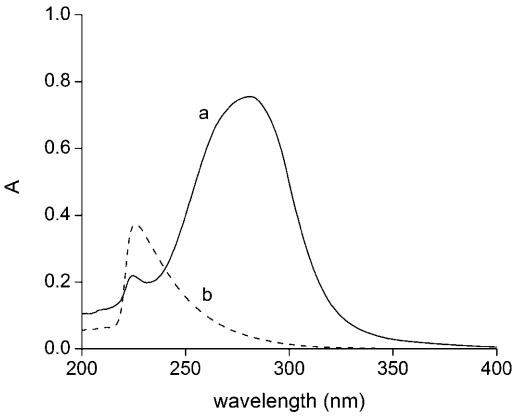


Figure 1. UV/Vis spectra of a) 50 μM $[Co(acac)_2]$ and b) 10 mM ROOH in cyclohexane at 343 K.

(Note that the band at $\lambda = 225$ nm was probably underestimated due to the decreased transparency of the sapphire windows below $\lambda = 220$ nm.) Although the latter signal from $[Co(acac)_2]$ interferes with the absorption by ROOH in this wavelength region (Figure 1), the consumption of ROOH can still be monitored by the absorbance signal at $\lambda =$ 225 nm, which is linear in [ROOH] (see the Supporting Information). It can indeed be expected that the concentrations of $Co^{II}$ ions and $Co^{III}$–OH remain virtually constant (quasi-steady-state) for the duration of the experiment so that spectral changes at $\lambda = 225$ nm can be mainly attributed to the consumption of ROOH.

As the absorption cross-section of the alcohols is much lower than that of ROOH and $[Co(acac)_2]$, the ROH product does not directly interfere in the spectroscopic measurements. Nevertheless, alcohols such as cyclohexanol (CyOH) seem to induce a significant blueshift when added to a solution of $[Co(acac)_2]$ in cyclohexane (Figure 2). The appearance of two isosbestic points ($\lambda = 280$ and 320 nm) demonstrates that under the experimental conditions, alcohols can coordinate to the cobalt ions. This behavior points either to the presence of vacant coordination sites in the $[Co(acac)_2]$ species or to a very rapid ligand-exchange reaction taking place. Given the high purity of the solvent and the hydrophilicity of cobalt ions, the most likely other ligand is water.

  

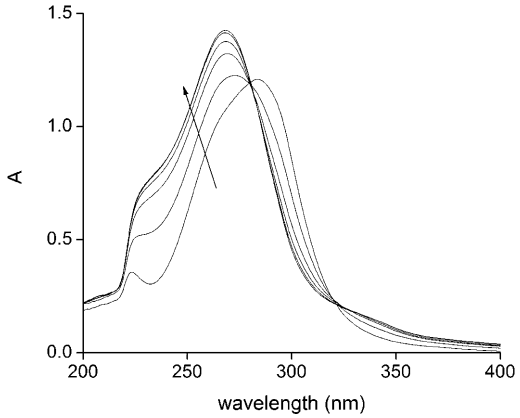


Figure 2. Effect of the addition of cyclohexanol (0, 20, 40, 60, 80, 100 mM) on the spectrum of 85 μM $[Co(acac)_2]$ at room temperature. Note the isosbestic points at $\lambda = 280$ and 320 nm.

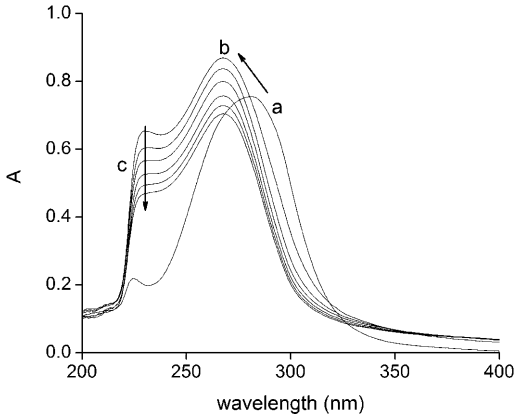


Figure 3. a) Spectrum of 50 μM $[Co(acac)_2]$ in CyH at 343 K. b) Instantaneous spectral shift upon the addition of 10.0 mM *tert*-butylhydroperoxide ($t = 0$), in part due to the coordination of $Co^{II}$ ions by ROOH. c) The subsequent decrease of absorbance as a function of time, which was uniform over the spectral range and due to the chemical removal of ROOH (spectra recorded every 60 s).

However, attenuated total reflection infrared (ATR-IR) measurements of the starting $[Co(acac)_2]$ powder showed no evidence for the presence of water. Moreover, the solubility of $H_2O$ is very low in CyH, thus rendering the possibility of additional water ligands (besides the acetylacetonate ligands) small. This hypothesis is supported by a similar and gradual blueshift in the $[Co(acac)_2]$ spectrum in CyH upon the addition of small quantities of water (in total below 100 mM), thus also leading to an isosbestic point at $\lambda =$ 277 nm. These observations suggest that the $[Co(acac)_2]$ species present in CyH have unoccupied coordination sites.

The coordination of alcohol is probably one of the main reasons why alcohols tend to inhibit cobalt-catalyzed autoxidation and deperoxidation reactions. Therefore, the deperoxidation of ROOH has to be studied under initial kinetic conditions, that is, at low conversions. The stability of the $[Co(acac)_2]$/methanol complex is computationally predicted to be 10.0 and 7.6 kcal mol$^{-1}$ at the UB3LYP/LANL2DZ and UBP86/LANL2DZ levels of theory, respectively. The fact that both DFT functionals - each with its own shortcomings - agree within a few kcal mol$^{-1}$ on the stability of the complex is an indication that this prediction is rather reliable. Moreover, the average stability of $\pm 9$ kcal mol$^{-1}$ is in qualitative agreement with the observed shift in Figure 2.

**Time-resolved measurements after the addition of ROOH**: The addition of ROOH to $[Co(acac)_2]$ in solution immediately induces similar spectroscopic changes as the addition of alcohol, thus indicating that ROOH also coordinates to the cobalt ions (Figure 3). Note that the initial strong increase of the absorption signal at around $\lambda = 230$ nm upon the addition of ROOH is caused by 1) ROOH itself and 2) coordination of ROOH to the $Co^{II}$ ion. Indeed, a comparison of Figures 1 and 3 shows that the absorbance of $[Co(acac)_2]$/ROOH in solution is greater (especially at around $\lambda = 250$ nm) than the algebraic sum of the absorbances of the two separate solutions. The stability of the $[Co(acac)_2]$/$CH_3OOH$ complex is computationally predicted to be 6.5 and 6.3 kcal mol$^{-1}$ at the UB3LYP/LANL2DZ[23] and UBP86/LANL2DZ[24] levels of theory, respectively. This finding is $\pm 2.5$ kcal mol$^{-1}$ weaker than for the alcohol complex. This relative difference seems to be significant, given the close agreement between the UB3LYP- and UBP86-predicted stabilities of both complexes. However, it was observed that a significantly smaller amount of ROOH can induce a similar spectroscopic shift than ROH. This observation could point towards the formation of other cobalt species that induce a similar blueshift (see below).

Immediately after the instantaneous spectral shift, the absorbance starts to decrease with time over the entire range $\lambda = 220$–350 nm due to consumption of ROOH (Figure 3). Although the absolute ROOH decay can not be measured due to the anticipated spectral interference of, for example, the $Co^{II}$/ROOH complex, the relative concentration of ROOH can still be followed because [$Co^{II}$/ROOH] is expected to be proportional to [ROOH]. The kinetic plots in Figure 4 unambiguously demonstrate first-order kinetics for ROOH. To avoid inhibition by coordination of the alcohol product to the cobalt species (see above), the reaction was monitored only until $[ROOH](t)/[ROOH](0) \approx 0.5$ (i.e., initial kinetics). As an example, the pseudo-first-order rate constant $k' \equiv -\mathrm{d}\ln\{[ROOH](t)/[ROOH](0)\}/\mathrm{d}t$ at 343 K with 50 μM $[Co(acac)_2]$ equals $2.0 \times 10^{-3}$ s$^{-1}$. Note that the absence of an induction period indicates that the species initially present are immediately active in the catalytic deperoxidation. Fast and irreversible catalyst deactivation can be excluded in the studied conversion range because the pseudo-first-order rate constants do not change as a function of time, that is, the slope of the plot of $\ln\{[ROOH](t)/[ROOH](0)\}$ versus time does not show any measurable decrease.

**Insight from quantum chemistry**: To gain more insight into the deperoxidation cycle, the potential-energy surfaces of reactions (1) and (2) were computationally characterized. It has to be emphasized that both reactions are very compli-

  

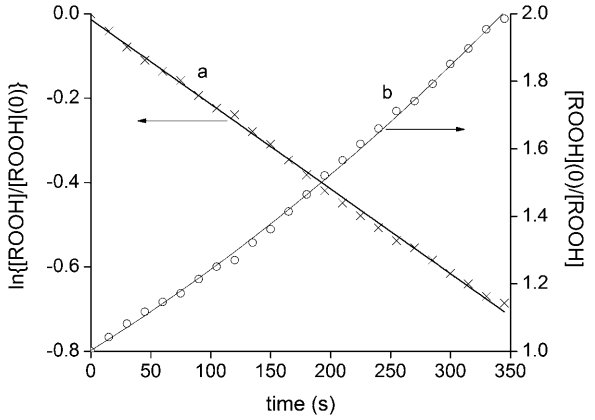


Figure 4. a) First-order and b) second-order kinetic plots of the deperoxidation of ROOH by 50 μM $[Co(acac)_2]$ at 343 K; [ROOH](0) = 10.0 mM. Determination of the pseudo-first-order rate constant $k' \equiv -d\ln\{[ROOH](t)/[ROOH](0)\}/dt = 2.0 \times 10^{-3}\ s^{-1}$.

cated from a computational point of view. Indeed, reliable calculations on transition-metal ions are very demanding, and the best approaches (such as full configuration interaction) are beyond our present computational resources for species of this size. A fairly reliable method, still feasible for the systems in hand, is the use of single-point UCCSD(T)[25] calculations on a preoptimized geometry. However, these calculations are still very demanding and cannot be applied to compute the energy of the involved transition states of reactions (1) and (2), which contain over 20 heavy atoms (i.e., C, O, and Co). Therefore, to decrease the computational efforts but still describe the active cobalt site appropriately, cobalt species in which the methyl groups in the acetylacetonate ligands were substituted by H atoms were used in combination with $CH_3OOH$, a smaller model hydroperoxide. In these preliminary calculations, it has moreover been assumed that the cobalt species are present as monomers without additional ligands (see above). The structure of the UB3LYP/LANL2DZ-optimized transition states is shown in Scheme 1 (Cartesian coordinates can be found in the Supporting Information).

These predictions suggest that reaction (1) is slightly slower than reaction (2), thus meaning that $[Co^{II}] \geq [Co^{III}–OH]$. This behavior could perhaps explain the initially observed spectral shift in the $[Co(acac)_2]$ spectrum upon the addition of ROOH. Indeed, despite the weaker interaction of ROOH with $[Co(acac)_2]$ than ROH (see above), the addition of ROOH affects the $[Co(acac)_2]$ spectrum already at much lower concentrations. It is therefore possible that the initial spectroscopic changes observed after the addition of ROOH to $[Co(acac)_2]$ in solution is only partially due to the coordination of ROOH to the $Co^{II}$ ion but mainly to the establishment of a quasi-steady-state concentration of $Co^{III}–OH$.

Although the substitution of H atoms for methyl groups seems justified in a first approximation, one should emphasize that the activation energy predicted with this model system (i.e., 19.9 kcal mol$^{-1}$) is probably a significant overestimation. Indeed, at the same level of theory (i.e., UCCSD(T)/LANL2DZ//UB3LYP/LANL2DZ), the energy of the reaction for the full acetylacetonate ligand system (i.e., with the methyl groups) was calculated to be −6.35 kcal mol$^{-1}$, that is, 12 kcal mol$^{-1}$ more exothermic than predicted with the smaller model in Table 1. Based on the correlation between the energy barrier and the energy of reaction (i.e., the Hammond principle or Evans–Polanyi correlations), the barrier of the rate-determining reaction (1) can be estimated to be 15 ± 3 kcal mol$^{-1}$. It should however be emphasized that a more-thorough computational study of the reaction-phase space is needed to understand the rich coordination chemistry of the cobalt ions during their catalytic cycle better. Such a study is however beyond the scope of this report.

Table 1. Relative energies (ZPE corrected) of stationary points along the reaction coordinate of reactions (1) and (2) at the UCCSD(T)/LANL2DZ//UB3LYP/LANL2DZ level of theory.[a]

| | Relative energies[b] [kcal mol$^{-1}$] |
|---|---|
| $Co^{II}$ + ROOH | 0.0 |
| $TS_{(1)}$ | 19.9 |
| $Co^{III}$–OH + RO$^{\cdot}$ | 5.8 |
| $Co^{III}$–OH + ROOH | 0.0 |
| $TS_{(2)}$ | 12.8[c] |
| $Co^{II}$–$OH_2$ + ROO$^{\cdot}$ | −15.3 |
| $Co^{II}$ + $H_2O$ + ROO$^{\cdot}$ | −1.4 |

[a] Calculations are based on the lowest spin states of $[Co(acac)_2]$ and $[Co(acac)_2]$–OH, namely, quartet and triplet, respectively. [b] Methyl groups in the acac ligands have been substituted by H atoms. [c] Note that in this calculation it was assumed that ROOH does not interact with the cobalt ion. Such an interaction actually decreases the barrier, however, it also increases the entropy of activation due to a more rigid transition state. Such effects are currently under investigation.

**Kinetic quantification at 323–343 K**: A number of measurements of the rate of ROOH removal was carried out at various concentrations of the $[Co(acac)_2]$ catalyst at three different temperatures (i.e., 323, 333, and 343 K; Figure 5). This plot demonstrates the first-order kinetics in the concentration of $[Co(acac)_2]$. The experiments were limited to 323–343 K because ROOH dimers could become important at lower $T$ values, whereas the reaction becomes too fast for

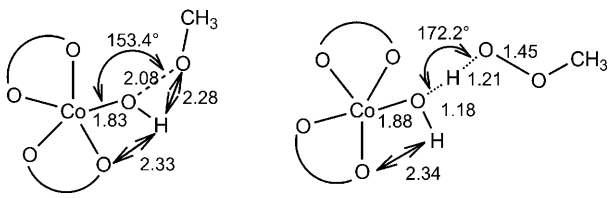


Scheme 1. Structure of the transition states of reactions (1) and (2), as predicted by UB3LYP/LANL2DZ for $CH_3OOH$ (the methyl groups in the acac ligands were substituted by H atoms; distances are given in Å). The unscaled imaginary frequencies equal $1313i^2$, and $1355i^2\ cm^{-1}$, respectively.

  

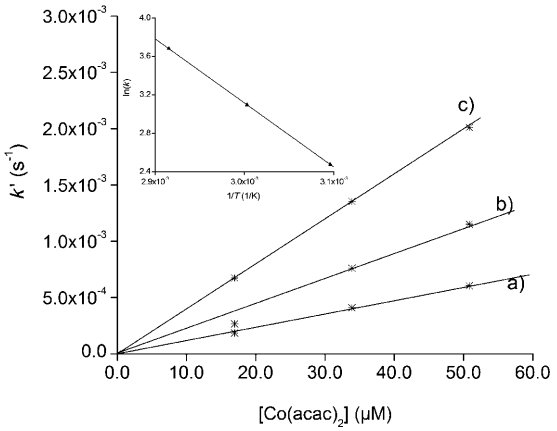


Figure 5. Pseudo-first-order rate constant for the deperoxidation of ROOH $k' \equiv -\mathrm{d}\ln\{[\mathrm{ROOH}](t)/[\mathrm{ROOH}](0)\}/\mathrm{d}t$ as a function of the [Co(acac)$_2$] catalyst concentration at different temperatures: a) 323, b) 333, and c) 343 K. The insert shows the Arrhenius plot of the apparent overall bimolecular rate coefficient $k(T)$.

accurate monitoring with the applied setup at higher $T$ values. However, this narrow $T$ range is compensated by the precision of the data. The apparent overall bimolecular rate coefficient $k(T)$ was obtained from the plots of $k' \equiv -\mathrm{d}\ln\{[\mathrm{ROOH}](t)/[\mathrm{ROOH}](0)\}/\mathrm{d}t$ versus [Co(acac)$_2$]. An Arrhenius plot of $\ln k(T)$ versus $1/T$ is inserted in Figure 5; the data can be fitted with excellent precision by the Arrhenius expression $k(T) = 1.2\times10^{10}\times\exp(-13\ \mathrm{kcal\,mol^{-1}}/RT)\ \mathrm{M^{-1}s^{-1}}$.

Although the measured Arrhenius activation energy of 13 kcal mol$^{-1}$ is in fair agreement with the predicted barrier of the rate-determining step (i.e., $15\pm3$ kcal mol$^{-1}$), the Arrhenius frequency factor (i.e., $A_{\mathrm{Arrh}} = 1.2\times10^{10}\ \mathrm{M^{-1}s^{-1}}$) is strikingly large. This outcome seems to indicate that the experimental findings are irreconcilable with the Haber–Weiss mechanism as the sole sink of ROOH, even allowing for the consumption of two additional ROOH molecules by the fast subsequent reactions (1) and (5) (see below). One must indeed conclude that the observed deperoxidation rate is approximately one order of magnitude higher than expected for a pure Haber–Weiss mechanism. The most probable rationalization is a chain mechanism initiated by the Haber–Weiss cycle.

**Reaction mechanism**: Rationalization of the experimental observations start by examination of the fate of the alkoxyl radicals produced in reaction (1). Radical RO$^\bullet$ can either react with the cyclohexane solvent [reaction (4)] or with the hydroperoxide [reaction (5)].

$$\mathrm{RO^\bullet + CyH \rightarrow ROH + Cy^\bullet} \quad (4)$$

$$\mathrm{RO^\bullet + ROOH \rightarrow ROH + ROO^\bullet} \quad (5)$$

The rate of reaction (4) was measured at 253–302 K;[26] slight extrapolation predicts $k_4$(333 K) to be as large as $(1.5\pm0.5)\times10^6\ \mathrm{M^{-1}s^{-1}}$. However, reactions of the type X$^\bullet$+ ROO–H→X–H+ROO$^\bullet$ are also known to be surprisingly fast.[27] Calculations at the UB3LYP/6-311++G(df,pd)// UB3LYP/6-31G(d,p) level, which are known to predict quantitatively reliable barriers for H-transfer reactions,[5] demonstrate that reaction (5) proceeds via a transition state (TS) that is located 2.95 kcal mol$^{-1}$ below the level of the reactants (a so-called submerged TS) due to the formation of strong pre- and post-reactive H-bonded complexes. The rate constant of reaction (5) predicted by TS theory (TST) would therefore be approximately $3\times10^{10}\ \mathrm{M^{-1}s^{-1}}$, given the average pre-exponential rate constant for H-transfer reactions of $3\times10^8\ \mathrm{M^{-1}s^{-1}}$.[8] This estimation of $k_5$ is one order of magnitude larger than the normal diffusion-controlled rate constant. Therefore, one has to estimate the precise rate at which the RO$^\bullet$ radical and ROOH diffuse towards each other, rather than using this TST value. Based on the long-range ROOH···OR dipole–dipole interaction and by adopting as a "reactive distance"—the separation of the reactants at which the interaction energy equals $k_BT$—the diffusion-limited rate constant $k_5$(333 K) can be estimated to be $2\times10^{10}\ \mathrm{M^{-1}s^{-1}}$.[28] This rate is significantly faster than diffusion-controlled reactions between nonpolar reactants in aqueous solutions (i.e., usually $\approx3\times10^9\ \mathrm{M^{-1}s^{-1}}$) but only slightly faster than, for example, the measured recombination of iodine atoms in hexane (i.e., $1.3\times10^{10}\ \mathrm{M^{-1}s^{-1}}$),[29] in which no long-range interactions are at play. The known or estimated rate constants of reactions (4) and (5) imply that under the experimental conditions (i.e., [CyH] = 9.5 M and initial [ROOH] = $10^{-2}$ M) the majority of the RO$^\bullet$ radicals react rapidly (within $\approx$3 ns) with ROOH to form ROO$^\bullet$ radicals and ROH. This conclusion is in line with Visser and coworkers, who studied the consumption of *tert*-butylhydroperoxide by *tert*-butoxyl radicals generated by the thermal dissociation of di-*tert*-butylperoxyoxalate at 318 K.[30]

We will return to the fate of the 5–10% Cy$^\bullet$ radicals formed in reaction (4). Furthermore, β-scission of the *tert*-butoxyl radical can be neglected in the experimental $T$ range.[26]

Note that when reaction (4) is neglected (see above), the rate-controlling reaction (1) and the two (fast) subsequent reactions (2) and (5) can be combined into one overall catalytic initiation reaction controlled by $k_1$ (i.e., $\mathrm{Co^{II} + ROOH\text{-}(+2\,ROOH) \rightarrow Co^{II} + ROH + H_2O + 2\,ROO^\bullet}$), with the rate of chain initiation (i.e., $R_{\mathrm{init}} = k_1[\mathrm{Co^{II}}][\mathrm{ROOH}]$; as a single chain involves two ROO$^\bullet$ radicals; see below), but with the rate of ROOH removal due to the initiation [Eq. (A)]:

$$(-\mathrm{d[ROOH]}/\mathrm{d}t)_{\mathrm{init}} = 3\,k_1[\mathrm{Co^{II}}][\mathrm{ROOH}] \quad (\mathrm{A})$$

For ROO$^\bullet$ radicals, two competing pathways are possible: the self-reactions (6a) and (6b) and the H-abstraction reaction with the solvent [reaction (7)].

$$\mathrm{ROO^\bullet + ROO^\bullet \rightarrow RO^\bullet + RO^\bullet + O_2} \quad (6a)$$

$$\mathrm{ROO^\bullet + ROO^\bullet \rightarrow ROOR + O_2} \quad (6b)$$

$$\mathrm{ROO^\bullet + CyH \rightarrow ROOH + Cy^\bullet} \quad (7)$$

The self-reaction of *tert*-butylperoxyl radicals—as is the case with all tertiary peroxyl radicals—produces mainly RO• radicals, whereas termination to form ROOR is only a minor channel, relative to the reactions of primary and secondary peroxyl radicals in which α-H atoms can be transferred.[1] Indeed, for tertiary peroxyl radicals, termination only occurs for a small fraction as a result of in-cage recombination of the nascent RO• radicals prior to their diffusive separation.[27] The total rate constant for the mutual reaction of two *tert*-butylperoxyl radicals in the gas phase is known to be $k_{6,gas}(333\,K) = 8\times10^{4}\,M^{-1}s^{-1}$.[31] In a noninteracting liquid, TST predicts the bimolecular rate constants to be approximately three times larger due to smaller translation partition functions of all the involved species in the liquid phase.[32] Therefore, a reasonable estimate of $k_6(333\,K)$ is approximately $3\times10^{5}\,M^{-1}s^{-1}$. This quantity is important because reaction (6a) becomes the rate-controlling propagation step in the overall mechanism of ROOH removal because each resulting RO• radical rapidly attacks an ROOH molecule through reaction (5). By attributing the observed deperoxidation rate (i.e., $1.1\times10^{-5}\,M\,s^{-1}$ at 50 μM $[Co(acac)_2]$ and 333 K; see above) mostly to the chain propagation (i.e., neglect the initiation as a sink for ROOH) and using the value of $k_{6a}\approx k_6$ (see above), [ROO•] can be estimated to be approximately $4\times10^{-6}$ M. The competing ROO• sink, namely, reaction (7), is characterized by the rate constant $k_7(333\,K)\approx3\times10^{-2}\,M^{-1}s^{-1}$.[3,33] Given the estimated [ROO•] of approximately $4\times10^{-6}$ M, the rate of reaction (7) should be close to $1.2\times10^{-6}\,M\,s^{-1}$. This value is approximately ten times smaller than the observed deperoxidation rate (i.e., $1.1\times10^{-5}\,M\,s^{-1}$), thus indicating that reaction (7) is only a minor sink for ROO• radicals (approximately 10%). Therefore, the rate-limiting propagation reaction (6a) can be, in a good approximation, combined with two times the subsequent reaction (5) into a single overall chain-propagation reaction (i.e., $ROO^{\bullet}+ROO^{\bullet}(+2\,ROOH)\rightarrow2\,ROH+O_2+2\,ROO^{\bullet}$) with chain-propagation rate (i.e., $R_{prop}=k_{6a}[ROO^{\bullet}]^2$; a single chain involving two ROO• chain propagators), but giving an rate of the ROOH removal by chain propagation (B):

$$(-d[ROOH]/dt)_{prop} = 2\,k_{6a}[ROO^{\bullet}]^2 \qquad (B)$$

According to this proposed mechanism (Scheme 2), the radical chain is not only propagated but also terminated by two ROO• radicals. Application of the radical quasi-steady-state, that is, equating the rate of chain initiation $R_{init}=k_I[Co^{II}][ROOH]$, to that of chain termination $R_{term}=k_{6b}[ROO^{\bullet}]^2$ leads to the expression (C) for the total ROOH removal rate: $-d[ROOH]/dt=(-d[ROOH]/dt)_{init}+(-d[ROOH]/dt)_{prop}$:

$$-d[ROOH]/dt = (3+2\,k_{6a}/k_{6b})\times k_1\times[Co^{II}]\times[ROOH] \qquad (C)$$

Thus, according to this chain mechanism, the experimentally observed rate coefficient $k(T)$ above is in fact $(3+2\,k_{6a}/k_{6b})\times k_1$. The chain length, defined as the ratio of the chain-propagation and chain-termination rates, simply equals $k_{6a}/k_{6b}$. This ratio has been experimentally determined to be (7—10):1 for *tert*-butylperoxyl radicals in benzene at 318 K.[30] A chain length on the order of 10, thus yielding $k(T)\approx20\times k_1$, appears reasonable, given that most of the nascent RO• radicals produced in the mutual reaction of ROO• will diffuse away from each other rather than combine. The temperature dependence of the $k_{6a}/k_{6b}$ ratio is expected to be small as it is controlled by diffusion, thus meaning that the experimentally observed activation energy of 13 kcal mol$^{-1}$ is a reasonable estimate for the energy barrier $E_b$ of reaction (1).

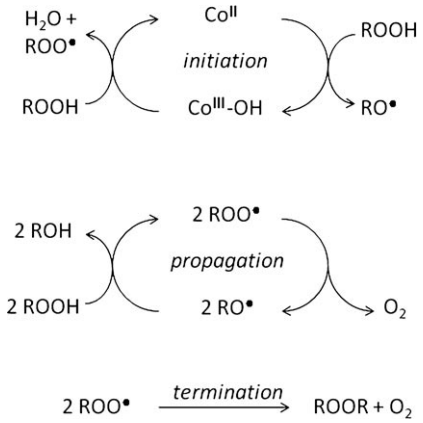


Scheme 2. The radical-chain mechanism responsible for the $Co^{II}$-induced decomposition of ROOH.

It is important to emphasize that Equation (C) correctly predicts the observed reaction orders for both cobalt and hydroperoxide. Many other mechanisms were considered, but all of them had to be rejected because they could either not explain the observed kinetics and/or the products observed in post-reaction analysis with gas chromatography (GC).

Under our conditions, the lifetime of ROOR is on the order of several days, that is, much longer than the timescale of the experiments. ROOR can thus be considered a true termination product. Experimental quantification of this compound, for example with GC, is very difficult given its low concentration and low stability in the GC injector (its lifetime at 473 K is only ≈1 s).

Although the general picture is clear and consistent, we have to return to the fate of the Cy• radicals formed in reactions (4) and (7). Despite our precautions to avoid $O_2$ in the system (by flushing the reactor with $N_2$), the formation of $O_2$ in situ cannot be avoided: about 0.5 $O_2$ is formed per ROOH consumed through reaction (6). Given that only approximately 0.15–0.2 Cy• radicals are expected to be generated per ROOH molecule removed, all Cy• radicals will be able to react with $O_2$, thus yielding the CyOO• radical. Indeed, with a diffusion-controlled rate constant of $3\times10^{9}\,M^{-1}s^{-1}$, the rate of Cy• loss, even at $[O_2]$ as low as $10^{-5}$ M, will still be as high as $3\times10^{4}\,s^{-1}$, far higher than any other Cy• radical reaction. Initially, at low ROOH conversions, the

  

CyOO$^{\bullet}$ peroxyl radicals will react mainly with ROOH and vice versa [reaction (8)]. This reaction is known to proceed with a rate constant of approximately $10^3\,\text{M}^{-1}\,\text{s}^{-1}$ at 303 K in both directions.[27]

$$\text{CyOO}^{\bullet} + \text{ROOH} \rightleftharpoons \text{CyOOH} + \text{ROO}^{\bullet} \quad (8)$$

So, after a short time the two types of peroxyl radicals will be in (pre-)equilibrium with $[\text{CyOO}^{\bullet}] \ll [\text{ROO}^{\bullet}]$ given that $[\text{ROOH}] \gg [\text{CyOOH}]$. Nevertheless, as the reaction proceeds, both CyOO$^{\bullet}$ and CyOOH will also start to react with the ROO$^{\bullet}$ radical and eventually also with cobalt, thus yielding cyclohexanol and cyclohexanone. However, the effective rate of CyOOH loss remains rather low due to its low concentration relative to ROOH, thus explaining why it can be detected by using GC. Significantly, the total amount of cyclohexane oxidation products observed with GC (i.e., $\pm 15\,\%$ with respect to *tert*-butyl alcohol) is in good agreement with the mechanism detailed above. This mechanism therefore also explains why the yield of the industrial deperoxidation of cyclohexylhydroperoxide in cyclohexane exceeds 100 % as one co-oxidizes a fraction of the cyclohexane solvent.

In summary, the mechanism shown in Scheme 2 is based on well-characterized reactions (experimentally and/or computationally) and can not only explain the observed reaction rate and reaction orders but also the minor fraction of cyclohexane oxidation products relative to the major product *tert*-butyl alcohol

**Mechanism at higher cobalt concentrations**: Although we seem to understand the chemistry at low cobalt concentrations, we are still faced with the challenge of rationalizing the very sudden decrease of the deperoxidation rate observed once $[\text{Co(acac)}_2] > 100\,\mu\text{M}$ (Figure 6).

Inhibition at higher cobalt concentrations has been known for a long time and was often ascribed to the high oxidizing power of ROO$^{\bullet}$ radicals, assumed to form a stable complex with the Co$^{\text{II}}$ catalyst:[1]

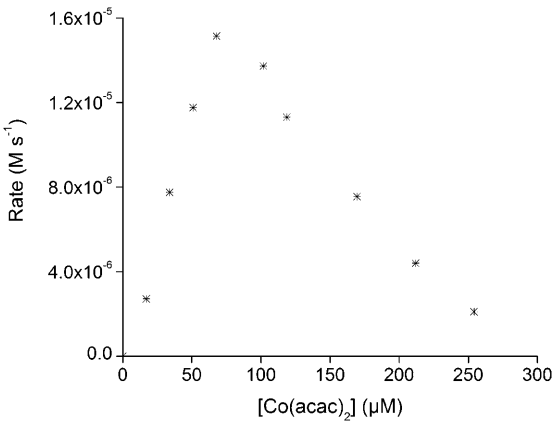


Figure 6. The observed rate of the decomposition of ROOH as a function of the total $[\text{Co(acac)}_2]$ concentration; $T = 333$ K.

$$\text{Co}^{\text{II}} + \text{ROO}^{\bullet} \rightleftharpoons \text{Co}^{\text{III}}\text{–OOR} \quad (9)$$

Therefore, excessive Co$^{\text{II}}$ ions would efficiently trap peroxyl radicals and hence interrupt the radical chain.[1,3,34] Although similar complexes have been synthesized,[35] the stability of the $[\text{Co(acac)}_2]$–OOR complex is probably insufficient to cause an irreversible removal of ROO$^{\bullet}$ radicals. Indeed, although the complex is predicted to be stable for 19.7 kcal mol$^{-1}$ at the UBP86/LANL2DZ level of theory, it is unstable at the UB3LYP/LANL2DZ level of theory. Given the opposite shortcomings of both consulted DFT functionals (i.e., B3LYP and BP86), a moderate stability should be concluded (i.e., between 0 and 20 kcal mol$^{-1}$). This peroxyl-trapping mechanism can therefore only cause a leveling of the overall rate at increasing cobalt concentrations, but it cannot cause inhibition, that is, a net decrease of the rate. Instead, one would approach a constant reaction rate, independent of the total cobalt concentration. Note that in case such a Co$^{\text{III}}$–OOR complex would be infinitely strong (i.e., even significantly stronger than predicted by UBP86/LANL2DZ), the catalyst would be irreversibly deactivated, which is in disagreement with the experimental observations (see above).

The sudden reversal of the dependence of the reaction rate on the cobalt concentration from a linear increase up to a value of $[\text{Co(acac)}_2] < 10^{-4}\,\text{M}$ to an abrupt decrease once $[\text{Co(acac)}_2] \geq 10^{-4}\,\text{M}$ is reached can only be explained by an additional and more efficient termination mechanism with the rate proportional to $[\text{Co}]^{\geq 2}$ but independent of [ROO$^{\bullet}$]. The latter condition is obvious: a dependence of the rate of the additional, faster termination mechanism on [ROO$^{\bullet}$] would induce negative feedback because enhanced termination necessarily decreases [ROO$^{\bullet}$]. As already pointed out, irreversible deactivation of the catalyst on the timescale of our experiments can also be excluded because this behavior would cause a decrease of the observed rate constant as a function of time, which is not observed up to 50 % conversion. This outcome implies that the cobalt species responsible for the enhanced termination must somehow be in steady state with the catalytically active cobalt species on the timescale of the experiments.

A hypothetical inhibition mechanism that is in line with the kinetic requirements above is now proposed. Its rate-controlling step is the association of two Co$^{\text{III}}$–OH species to form a strong dimer presumably the bis(μ-hydroxo) complex Co-(OH)$_2$-Co in which both cobalt species have an octahedral coordination [reaction (10) and Scheme 3].[36] Note that this proposition implies the assumption that the Co$^{\text{III}}$–OH species have a sufficient lifetime; that is, reaction (2) is not controlled by diffusion.

$$\text{Co}^{\text{III}}\text{–OH} + \text{Co}^{\text{III}}\text{–OH} \rightarrow \text{Co-(OH)}_2\text{-Co} \quad (10)$$

The UB3LYP/LANL2DZ and UBP86/LANL2DZ stabilities of this bis(μ-hydroxo) complex equal 46.9 and 43.3 kcal mol$^{-1}$, respectively. As a consequence, thermal dissociation of this complex is very slow under the given conditions. Ac-

  

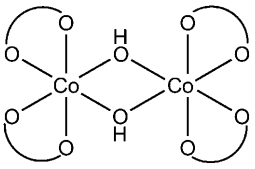

Scheme 3. Proposed structure of the bis(μ-hydroxo) dimer formed upon the combination of two $Co^{III}$–OH species.

tually, the most likely fate of this complex is its reaction with the chain-propagating ROO• radicals, present at a high concentration. One possibility is, for example, that ROO• radicals would abstract the H atoms of the bridging hydroxo ligands [reactions (11) and (12)].

$$Co\text{-}(OH)_2\text{-}Co + ROO^{\bullet} \rightarrow Co\text{-}(OH)(O)\text{-}Co + ROOH \quad (11)$$

$$Co\text{-}(OH)(O)\text{-}Co + ROO^{\bullet} \rightarrow Co\text{-}(O_2)\text{-}Co + ROOH \quad (12)$$

The resulting Co-($O_2$)-Co peroxo complex is likely to dissociate spontaneously into two $Co^{II}$ ions plus molecular oxygen,[37] driven by the bond strength in $O_2$ of 119 kcal mol$^{-1}$:

$$Co\text{-}(O_2)\text{-}Co \rightarrow 2\,Co^{II} + O_2 \quad (13)$$

To regenerate the $Co^{II}$ species on the timescale of the experiments, the barriers of reactions (11) and (12) should be smaller than 7 kcal mol$^{-1}$ given $[ROO^{\bullet}] \approx 4 \times 10^{-6}$ M (see above) and an estimated pre-exponential rate factor of approximately $10^8$ M$^{-1}$ s$^{-1}$. At the UB3LYP/LANL2DZ level of theory, the barrier of reaction (11) is predicted to be 12.2 kcal mol$^{-1}$. However, this prediction is probably an overestimation of the true barrier as a scan along the reaction coordinate at the UBP86/LANL2DZ level of theory remains energetically below the reactants level.

The sequence that consists of reactions (11) and (12) removes two ROO• radicals, thus canceling the effect of the fast initiation (i.e., $Co^{II} + 3\,ROOH \rightarrow Co^{II} + ROH + H_2O + 2\,ROO^{\bullet}$). However, the rate of this additional chain-termination mechanism is kinetically independent of [ROO•] because its rate is solely controlled by the second-order $Co^{III}$–OH association reaction (10). Note that reaction (10) is in direct competition with the chain-initiation reaction (2), that is, first order in the concentration of [$Co^{III}$–OH]. It is readily shown that under the assumptions made, the rate of radical chain propagation $(-d[ROOH]/dt)_{prop}$ will show a maximum as a function of the $Co^{III}$–OH concentration, and the peak rate will occur according to Equation (D):

$$k_1[Co^{II}][ROOH] = 2\,k_{10}[Co^{III}\text{–}OH][Co^{III}\text{–}OH] \quad (D)$$

Further experimental support for the proposed inhibition mechanism was found in the study of the analogous, though sterically hindered bis(2,2,6,6-tetramethyl-3,5-heptanedionato)cobalt(II) complex (Scheme 4). The UBP86/LANL2DZ

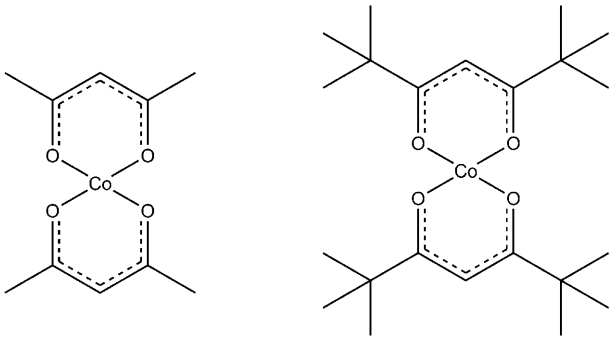

Scheme 4. Structure of bis(acetylacetonato)cobalt(II) (left) and the analogous, though sterically hindered, bis(2,2,6,6-tetramethyl-3,5-heptanedionato)cobalt(II) species (right).

-computed stability of the analogous bis(μ-hydroxo) complex was 36.6 kcal mol$^{-1}$, that is, only 6.7 kcal mol$^{-1}$ less than for the [Co(acac)$_2$] system. Nevertheless, bis(2,2,6,6-tetramethyl-3,5-heptanedionato)cobalt(II) behaves totally different in the deperoxidation of ROOH: irreversible catalyst deactivation is observed. Indeed, the activity slows down to zero after a few turnovers. This observation can readily be explained by the above mechanism. The bridging hydroxyl groups in the bis-(μ-hydroxo) complex of bis(2,2,6,6-tetramethyl-3,5-heptanedionato)cobalt(II) are not accessible for peroxyl radicals, thus meaning that the active form of the catalyst cannot be regenerated. Every time two $Co^{III}$–OH species combine, the active catalyst concentration decreases irreversibly.

Although the proposed mechanism predicts the net decrease of the reaction rate and the observed first-order kinetics of ROOH, the observed changeover from an increase to a decrease of the reaction rate as a function of the cobalt concentration is more abrupt than solely predicted by this mechanism. Probably there is a synergic effect of an increasing fraction of the chain-propagating ROO• radicals that oxidize $Co^{II}$ ions to $Co^{III}$–OOR [reaction (9)]. Another effect that likely decreases the deperoxidation rate at higher cobalt concentrations further is the association of the [Co(acac)$_2$] species. Experimental evidence for the formation of cobalt dimers can be found in the shift of the absorption maximum in UV/Vis spectra to higher wavelengths at higher cobalt concentrations (i.e., >75 μM). At the UBP86/LANL2DZ level of theory, the formation of such [{Co(acac)$_2$}$_2$] dimers is predicted to be favored by 6.6 kcal mol$^{-1}$. In these dimers, one Co center is surrounded by six oxygen atoms from the acac ligands, whereas the other Co center is surrounded by only five oxygen atoms, thus leaving one coordination site available (see the Supporting Information). Although it is likely that these cobalt dimers can still react with ROOH and initiate the radical chain, dimerization causes a decrease of the available active sites.

In summary, the $Co^{III}$–OH species can probably either cause first-order chain initiation upon reaction with ROOH or second-order chain termination upon their mutual reaction at increasing cobalt concentrations (Scheme 5). Which

  

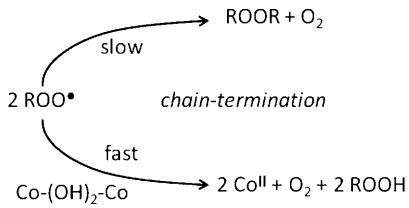


Scheme 5. Different termination mechanisms during the catalytic decomposition of ROOH. Upper: normal mutual termination reaction between two ROO• radicals; lower: termination catalyzed by Co dimers at high catalyst concentrations.

of these two mechanisms dominates is determined by the overall catalyst concentration.

## Conclusion

Herein, the catalytic deperoxidation of *tert*-butylhydroperoxide with $[Co(acac)_2]$ was studied by in situ UV/Vis spectroscopic analysis at 323–343 K. It is proposed that a Haber–Weiss mechanism is responsible for the initiation of a radical-chain mechanism propagated by alkoxyl and peroxyl radicals. The absence of an efficient termination channel in the mutual reaction of tertiary peroxyl radicals results in a chain length on the order of 10. The majority of the hydroperoxide radicals are therefore destroyed by propagation reactions rather than the Haber–Weiss cycle. At higher $[Co(acac)_2]$ concentrations, strong inhibition of the radical chain is observed, thus causing a net decrease of the deperoxidation rate. This behavior is kinetically in line with a proposed mutual termination reaction of the $Co^{III}$–OH species at high catalyst concentrations, thus leading to a stable bis(μ-hydroxo) dimer. This complex is proposed to react exclusively with chain-carrying peroxyl radicals, thus leading to a pronounced reduction in the net deperoxidation rate. Although this additional termination mechanism slows down the net deperoxidation rate even in a drastic way, it does not cause an irreversible deactivation because it regenerates the catalytically active $Co^{II}$ species. It is our aim to further characterize this reaction (both experimentally and computationally) and to investigate the influence of the ligands and additives. Also the performance of heterogeneous catalytic systems will be compared and rationalized in the light of the proposed mechanism.

## Experimental Section

In the experimental setup, the light of a deuterium–halogen source was guided by optical fibers to a magnetically stirred high-pressure reactor (10 mL). The light was passed through the reactor (optical path length: ≈1 cm) through sapphire windows and guided to an Ocean Optics USB2000 spectrometer through a second optical fiber. The integration time of the CCD detector was set at 5 ms, thus averaging out 100 spectra to improve the signal-to-noise ratio. A dark spectrum was recorded with a closed light shutter, while reference spectra were recorded with only cyclohexane in the reactor. The reaction was initiated by adding a known quantity of a prediluted ROOH in cyclohexane (0.275 M) to an $N_2$-flushed solution of $[Co(acac)_2]$ in CyH (5 mL) in the reactor, after which the reaction was monitored under an $N_2$ atmosphere. All the studied cobalt solutions were obtained from the same mother solution (1.0 mM $[Co(acac)_2]$ in cyclohexane) through dilution with $N_2$-flushed cyclohexane. Note that the sapphire windows of the high-pressure reactor absorb light below $\lambda \leq$ 220 nm, thus deforming the far-UV range of the spectrum.

Quantum-chemical calculations were performed with the Gaussian03 software[38] at the indicated level of theory. The reported relative energies of the stationary points on the potential-energy surfaces (ie., energy barriers $E_b$ and reaction energies $\Delta E$) were corrected for ZPE differences.

## Acknowledgements

Financial support from the Swiss National Science foundation (grant 200021 124698) and the ETH Zurich is kindly acknowledged by the authors. I.H. is grateful for the granted Chemical European Science and Engineering Award 2009 from ExxonMobil.

[1] R. A. Sheldon, J. K. Kochi, *Metal-Catalyzed Oxidations of Organic Compounds*, Academic Press, Amsterdam, **1981**.
[2] C. A. Tolman, J. D. Druliner, M. J. Nappa, N. Herron in *Activation and Functionalization of Alkanes* (Ed.: C. L. Hill), Wiley, New York, **1989**.
[3] G. Franz, R. A. Sheldon, *Oxidation, Ullmann's Encyclopedia of Industrial Chemistry*, Wiley-VCH, Weinheim, **2000**.
[4] a) S. Bhaduri, D. Mukesh, *Homogeneous Catalysis, Mechanisms and Industrial Applications*, Wiley, New York, **2000**; b) I. Hermans, E. S. Spier, U. Neuenschwander, N. Turrà, A. Baiker, *Top. Catal.* **2009**, *52*, 1162; c) F. Cavani, J. H. Teles, *ChemSusChem* **2009**, *2*, 508.
[5] I. Hermans, T. L. Nguyen, P. A. Jacobs, J. Peeters, *ChemPhysChem* **2005**, *6*, 637.
[6] I. Hermans, P. A. Jacobs, J. Peeters, *J. Mol. Catal. A* **2006**, *251*, 221.
[7] I. Hermans, J. Peeters, L. Vereecken, P. Jacobs, *ChemPhysChem* **2007**, *8*, 2678.
[8] I. Hermans, J. Peeters, P. Jacobs, *J. Org. Chem.* **2007**, *72*, 3057.
[9] I. V. Berezin, E. T. Denisov, N. M. Emanuel, *The Oxidation of Cyclohexane*, Pergamon Press, New York, **1966**.
[10] M. T. Musser, *Cyclohexanol and Cyclohexanone, Ullmann's Encyclopedia of Industrial Chemistry*, Wiley-VCH, Weinheim, **2000**.
[11] See, for example: a) G. Olason, D. C. Sherrington, *React. Funct. Polym.* **1999**, *42*, 163; b) M. Salavati-Niasari, F. Farzaneh, M. Ghandi, *J. Mol. Catal. A* **2002**, *186*, 101; c) A. Chica, G. Gatti, B. Moden, L. Marchese, E. Iglesia, *Chem. Eur. J.* **2006**, *12*, 1960; d) H. E. B. Lempers, R. A. Sheldon, *Stud. Surf. Sci. Catal.* **1997**, *110*, 557, edited by R. K. Grasselli, S. T. Oyama, A. M. Gaffney, J. E. Lyons; e) K. Kervinen, H. Korpi, J. G. Mesu, F. Soulimani, T. Repo, B. Rieger, M. Leskelä, B. M. Weckhuysen, *Eur. J. Inorg. Chem.* **2005**, 2591.
[12] a) S. Tanase, E. Bouwman, J. Reedijk, *Appl. Catal. A* **2004**, *259*, 101; b) R. van Gorkum, E. Bouwman, *Coord. Chem. Rev.* **2005**, *249*, 1709.
[13] a) F. Haber, J. Weiss, *Naturwissenschaften* **1932**, *20*, 948; b) F. Haber, J. Weiss, *Proc. R. Soc. London Ser. A* **1934**, *147*, 332; c) G. Sosnovsky, D. J. Rawlinson in *Organic Peroxides, Vol. 2* (Ed.: D. Swern), Wiley, New York, **1971**, p. 153; d) R. A. Sheldon, J. K. Kochi, *Adv. Catal.* **1976**, *25*, 272; e) S. Goldstein, D. Meyerstein, *Acc. Chem. Res.* **1999**, *32*, 547; f) W. H. Koppenol, *Redox Rep.* **2001**, *6*, 229.
[14] G. W. Parshall, S. D. Ittel, *Homogeneous Catalysis: the Applications and Chemistry of Catalysis by Soluble Transition Metal Complexes*, 2nd ed., Wiley, New York, **1992**.
[15] Yu. S. Zimin, E. P. Talzi, V. M. Nekipelov, V. D. Chinakov, K. I. Zamaraev, *React. Kinet. Catal. Lett.* **1985**, *29*, 225.
[16] N. A. Johnson, E. S. Gould, *J. Am. Chem. Soc.* **1973**, *95*, 5198.

  

[17] a) E. J. Y. Scott, *J. Phys. Chem.* **1970**, *74*, 1174; b) R. Prikryl, A. Tkac, L. Malik, L. Omelka, K. Vesely, *Collect. Czech. Chem. Commun.* **1975**, *40*, 104; c) R. P. Houghton, C. R. Rice, *Polyhedron* **1996**, *15*, 1893; d) P. G. Harris, R. P. Houghton, P. L. Taylor, *Polyhedron* **1997**, *16*, 2651.

[18] C. A. Tolman, J. D. Druliner, P. J. Krusic, M. J. Nappa, W. C. Seidel, I. D. Williams, S. D. Ittel, *J. Mol. Catal.* **1988**, *48*, 129.

[19] F. Minisci, F. Recupero, G. F. Pedulli, M. Lucarini, *J. Mol. Catal. A* **2003**, *204*, 63.

[20] a) R. A. Sheldon, M. Wallau, I. W. C. E. Arends, U. Schuchardt, *Acc. Chem. Res.* **1998**, *31*, 485; b) R. A. Sheldon, I. W. C. E. Arends, H. E. B. Lempers, *Catal. Today* **1998**, *41*, 387; c) B. Moden, B. Z. Zhan, J. Dakka, J. G. Santiesteban, E. Iglesia, *J. Phys. Chem. C* **2007**, *111*, 1402; d) B. Z. Zhan, B. Moden, J. Dakka, J. G. Santiesteban, E. Iglesia, *J. Catal.* **2007**, *245*, 316; e) B. Moden, B. Z. Zhan, J. Dakka, J. G. Santiesteban, E. Iglesia, *J. Catal.* **2006**, *239*, 390; f) B. Modén, L. Oliviero, J. Dakka, J. G. Santiesteban, E. Iglesia, *J. Phys. Chem. B* **2004**, *108*, 5552; g) F. X. L. i Xamena, O. Casanova, R. G. Tailleur, H. Garcia, A. Corma, *J. Catal.* **2008**, *255*, 220.

[21] a) S. S. Ivanchev, P. I. Selivanov, V. V. Konovalenko, *J. Appl. Spectrosc.* **1975**, *22*, 877; b) O. P. Yablonskii, N. S. Lastochkina, V. A. Belyayev, *Pet. Chem. USSR* **1973**, *13*, 261; O. P. Yablonskii, N. S. Lastochkina, V. A. Belyayev, *Neftekhimiya* **1973**, *13*, 851.

[22] Y. Zhao, D. G. Truhlar, *J. Phys. Chem. A* **2005**, *109*, 4209.

[23] a) A. D. Becke, *J. Chem. Phys.* **1992**, *96*, 2155; A. D. Becke, *J. Chem. Phys.* **1992**, *97*, 9173; A. D. Becke, *J. Chem. Phys.* **1993**, *98*, 5648; b) C. Lee, W. Yang, R. G. Parr, *Phys. Rev. B* **1988**, *37*, 785.

[24] a) J. P. Perdew, *Phys. Rev. B* **1986**, *33*, 8822; b) J. P. Perdew, *Phys. Rev. B* **1986**, *34*, 7046.

[25] J. A. Pople, M. Head-Gordon, K. Raghavachari, *J. Chem. Phys.* **1987**, *87*, 5968.

[26] M. Weber, H. Fischer, *J. Am. Chem. Soc.* **1999**, *121*, 7381.

[27] K. U. Ingold, *Acc. Chem. Res.* **1969**, *2*, 1.

[28] S. W. Benson, *The Foundations of Chemical Kinetics*, McGraw-Hill, New York, **1960**.

[29] a) E. Rabinowitch, W. C. Wood, *Trans. Faraday Soc.* **1936**, *32*, 547; b) S. Aditya, J. E. Willard, *J. Am. Chem. Soc.* **1957**, *79*, 2680.

[30] R. Hiatt, J. Clipsham, T. Visser, *Can. J. Chem.* **1964**, *42*, 2754.

[31] R. Atkinson, D. L. Baulch, R. A. Cox, R. F. Hampson, J. A. Kerr, M. J. Rossi, J. Troe, *J. Phys. Chem. Ref. Data* **1997**, *26*, 1329.

[32] C. Canepa, M. Mosso, A. Maranzana, G. Tonachini, *Eur. J. Org. Chem.* **2005**, 342.

[33] J. A. Howard in *Peroxyl Radicals* (Ed.: Z. Alfassi), Wiley, New York, **1997**.

[34] J. F. Black, *J. Am. Chem. Soc.* **1978**, *100*, 527.

[35] a) F. A. Chavez, C. V. Nguyen, M. M. Olmstead, P. K. Mascharak, *Inorg. Chem.* **1996**, *35*, 6282; b) F. A. Chavez, P. K. Mascharak, *Acc. Chem. Res.* **2000**, *33*, 539.

[36] a) J. Springborg in *Advances in Inorganic Chemistry, Vol. 32* (Ed.: A. G. Sykes), Academic Press, San Diego, **1988**; b) C. He, S. J. Lippard, *J. Am. Chem. Soc.* **1998**, *120*, 105; c) S. Hikichi, H. Komatsuzaki, N. Kitajima, M. Akita, M. Mukai, T. Kitagawa, Y. Moro-oka, *Inorg. Chem.* **1997**, *36*, 266; d) K. Nakamoto, *Infrared and Raman Spectra of Inorganic and Coordination Compounds, Part B: Applications in Coordination, Organometallic and Bioinorganic Chemistry*, Wiley, New York, **1997**.

[37] a) R. MacArthur, A. Sucheta, F. F. Chong, O. Einarsdóttir, *Proc. Natl. Acad. Sci. USA* **1995**, *92*, 8105; b) H. Nishide, H. Yoshioka, S.-G Wang, E. Tsuchida, *Makromol. Chem.* **1985**, *186*, 1513.

[38] Gaussian 03, Revision D.01, M. J. Frisch, G. W. Trucks, H. B. Schlegel, G. E. Scuseria, M. A. Robb, J. R. Cheeseman, J. A. Montgomery, Jr., T. Vreven, K. N. Kudin, J. C. Burant, J. M. Millam, S. S. Iyengar, J. Tomasi, V. Barone, B. Mennucci, M. Cossi, G. Scalmani, N. Rega, G. A. Petersson, H. Nakatsuji, M. Hada, M. Ehara, K. Toyota, R. Fukuda, J. Hasegawa, M. Ishida, T. Nakajima, Y. Honda, O. Kitao, H. Nakai, M. Klene, X. Li, J. E. Knox, H. P. Hratchian, J. B. Cross, V. Bakken, C. Adamo, J. Jaramillo, R. Gomperts, R. E. Stratmann, O. Yazyev, A. J. Austin, R. Cammi, C. Pomelli, J. W. Ochterski, P. Y. Ayala, K. Morokuma, G. A. Voth, P. Salvador, J. J. Dannenberg, V. G. Zakrzewski, S. Dapprich, A. D. Daniels, M. C. Strain, O. Farkas, D. K. Malick, A. D. Rabuck, K. Raghavachari, J. B. Foresman, J. V. Ortiz, Q. Cui, A. G. Baboul, S. Clifford, J. Cioslowski, B. B. Stefanov, G. Liu, A. Liashenko, P. Piskorz, I. Komaromi, R. L. Martin, D. J. Fox, T. Keith, M. A. Al-Laham, C. Y. Peng, A. Nanayakkara, M. Challacombe, P. M. W. Gill, B. Johnson, W. Chen, M. W. Wong, C. Gonzalez, J. A. Pople, Gaussian, Inc., Wallingford CT, **2004**.

Received: February 24, 2010
Revised: June 25, 2010
Published online: October 13, 2010

  